FPGA Based ESC and IMU

for

Mini Project – II

of

Third Year (Semester-VI)

Bachelors in Engineering

by

Group Name: ByteBlitzers

Shardul Bhave	**D14A (03)**
Rahul Desai	**D14A (11)**
Jaishree Epili	**D14A (16)**

Supervisor

Prof. Mrugendra Vasmatkar

Assistant Professor

Department of Electronics, and Telecommunication Engineering

Vivekan, and Education Society's Institute of Technology

An Autonomous Institute Affiliated to University of Mumbai

AY-2024-2025

Mini Project-II Approval

Project titled **FPGA based ESC and IMU** by **Shardul Bhave, Rahul Desai, and Jaishree Epili** is approved for the Third year of Engineering.

Examiners

1. _____

Internal

2. _____

External

Supervisor

1. _____

Date:

Place:

Certificate

This is to certify that **Shardul Bhave, Rahul Desai, and Jaishree Epili** have completed the project report on the topic **FPGA based ESC and IMU** satisfactorily in partial fulfillment of the requirements for Mini Project II of Third Year, (Semester-VI) in Electronics, and Telecommunication under the guidance of **Mr. Mrugendra Vasmatkar** during the year 2024-2025.

Supervisor	**Head of Department**
Mr. Mrugendra Vasmatkar	**Dr. Chandan Singh Rawat**

Principal
Dr. Jayalekshmi Nair

Examiner 1	**Examiner 2**

Declaration

We declare that this written submission represents our ideas in our words, and where others' ideas or words have been included, we have adequately cited, and referenced the original sources. We also declare that we have adhered to all principles of academic honesty, and integrity, and have not misinterpreted or fabricated or falsified any idea/data/fact/source in my submission. We understand that any violation of the above will be cause for disciplinary action by the Institute, and can also evoke penal action from the sources which have thus not been properly cited or from whom proper permission has not been taken when needed.

_____

SHARDUL BHAVE

_____

RAHUL DESAI

_____

JAISHREE EPILI

Date:

Table of Contents

Table of Figures

Abstract

This report presents the design and implementation of an advanced FPGA-based Inertial Measurement Unit (IMU) and Electronic Speed Controller (ESC) system, developed using a Boolean board as the hardware platform. The IMU subsystem leverages Xilinx's MicroBlaze soft-core processor IP to efficiently manage sensor data acquisition and processing. It incorporates the MPU6050 sensor for high-precision 3-axis accelerometer and gyroscope measurements, along with the BMP280 barometric pressure sensor to enable altitude estimation—a critical parameter for UAV navigation and stabilization. To ensure robust and accurate sensor fusion, the system implements a complementary filter for real-time data processing, effectively combining accelerometer and gyroscope readings to compute stable orientation estimates (roll, pitch, and yaw). For comparative validation, a Kalman filter is employed as a benchmark, demonstrating the system's capability to handle sensor noise and dynamic environmental conditions with high reliability. The ESC module, designed alongside the IMU, provides closed-loop motor control for BLDC motors, featuring PWM generation, back-EMF sensing, and dynamic speed adjustment—all implemented in FPGA hardware for low-latency performance. By integrating both IMU and ESC functionalities on a single FPGA platform, this project highlights the advantages of hardware-accelerated processing for real-time embedded systems.

Chapter 1

Introduction

In recent years, the dem, and for precision motion control in various applications, such as robotics, drones, and autonomous vehicles, has intensified. Central to these systems is the Inertial Measurement Unit (IMU), which provides critical data about an object's orientation, acceleration, and velocity. This project focuses on the design, and implementation of an FPGA-based IMU using the ZYBO board, integrating multiple sensors to enhance the accuracy, and reliability of motion data.

The IMU in this project comprises the MPU6050, which captures three-dimensional acceleration, and angular velocity. Additionally, the BMP280 sensor measures atmospheric pressure, aiding in altitude estimation, while the HMC5883L magnetometer provides heading direction for improved orientation tracking. To address sensor noise, and inaccuracies, a Kalman filter is implemented for sensor fusion, ensuring smooth, and reliable motion estimation.

By utilizing FPGA technology, and VIVADO SDK, the system achieves high processing speeds, and real-time sensor data acquisition, making it well-suited for embedded motion control applications. This report details the design, implementation, and evaluation of the FPGA-based IMU, and Electronic Speed Controller (ESC), demonstrating the advantages of FPGA-based motion control systems in terms of efficiency, accuracy, and adaptability.

Problem Statement

Developing an FPGA-based ESC, and IMU system for UAVs enhances flight stability, control, and efficiency. The ESCs use FPGA technology for precise motor regulation, while the IMU integrates advanced sensors for accurate attitude measurement. Key goals include low-latency communication, parallel processing, and efficient motor operation. The system's scalability ensures integration across various UAV platforms, with a focus on reliability, and safety through rigorous testing.

Chapter 2

Review of Literature

This chapter serves as an introduction to the report, offering an overview of existing knowledge, and research in the field. It sets the stage by highlighting key findings, trends, and gaps, providing context for the research's placement, and intended contributions. The survey succinctly communicates what has been studied, current knowledge, and the specific questions or areas the report aims to address.

"Inertial Measurement Unit Error Modeling: Inertial Navigation System State Estimation with Real-Time Sensor Calibration" presents a detailed guide on modelling stochastic errors in IMUs to improve inertial navigation system (INS) accuracy. It emphasizes the importance of sensor fusion in autonomous systems, where high-frequency IMU data is combined with aiding sensors like GNSS, lidar, and cameras using estimation techniques such as Kalman filters. The paper introduces the concept of real-time calibration by incorporating IMU error models into state estimators through state augmentation. Starting from manufacturer-provided Allan Variance (AV) or Allan Standard Deviation (ASD) plots, the authors guide readers in constructing continuous-time stochastic error models, and converting them into discrete-time state-space models suitable for implementation. These models simulate error behavior, and align their statistical output with real AV/ASD data. A simplified 2D INS example explains nonlinear vehicle dynamics, and illustrates calibration in action. The tutorial also reviews the historical evolution of INS from gimballed to strapdown systems, and discusses various aiding strategies like tight, and loose coupling. It underscores the challenges of modeling stochastic processes due to the lack of raw IMU data, and the non-uniqueness of models. Practical MATLAB tools accompany the tutorial for model fitting, and AV simulation. The paper concludes that while no universal model exists, understanding AV-based modeling is crucial for accurate, robust navigation. It provides a foundation for developing efficient, industry-standard IMU error models.[1]

"Robust Vehicular Localization, and Map Matching in Urban Environments Through IMU, GNSS, and Cellular Signals" presents a localization framework designed for urban areas where GNSS signals are often unreliable due to obstructions like buildings. This system integrates

data from Inertial Measurement Units (IMUs), GNSS, and cellular Signals of Opportunity (SOPs), utilizing an Extended Kalman Filter (EKF) to fuse these inputs with digital map data. By assuming known positions of cellular towers, the framework estimates the vehicle's position, velocity, orientation, and IMU biases, along with clock errors between the vehicle's receiver, and each cellular SOP. Experimental results demonstrate that this approach achieves a root-mean-square error (RMSE) of 2.8 meters over a 1,380-meter trajectory when GNSS is available, and 3.12 meters even when GNSS is unavailable for 330 meters. Compared to traditional GNSS-IMU systems, this method reduces localization errors by 22% with GNSS, and by 81% without GNSS, highlighting its robustness in challenging urban environments.[2]

"Design, and Performance Analysis of Electrical Vehicle Using BLDC Motor, and Bidirectional Converter" presents the design, and performance analysis of an electric vehicle (EV) powered by a BLDC motor, and a bidirectional converter. The bidirectional converter allows for energy regeneration during braking, increasing the overall efficiency of the system. The authors analyze the performance of the EV under various conditions, focusing on acceleration, power consumption, and energy recovery. The paper demonstrates that using a BLDC motor in combination with the bidirectional converter can significantly improve the energy efficiency of the vehicle, reduce energy losses, and lower operational costs, making it a viable solution for electric vehicle propulsion systems.[3]

"Sensorless Brushless DC Motor Drive Based on the Zero-Crossing Detection of Back Electromotive Force (EMF)" explores a sensorless control method for BLDC motors based on detecting the zero-crossing points of the back EMF. Traditionally, BLDC motor controllers rely on position sensors to detect the rotor’s position, which increases cost, and system complexity. This paper presents a sensorless technique where the back EMF is measured directly to infer the rotor’s position. This method eliminates the need for additional sensors, making the system more cost-effective, and reliable. The authors validate the technique through simulations, and experimental results, showing that it provides precise control without the need for sensors.[4]

"Serrani andrea (2025) - Technical Committee on Nonlinear Systems, and Control [Technical Activities]" discusses the activities of the Technical Committee on Nonlinear Systems, and Control. It focuses on advancing research, and applications in nonlinear control systems, which are essential in many real-world phenomena, such as robotics, and aerospace. The paper

reviews current research trends, emerging methodologies, and practical applications in nonlinear systems. It emphasizes the importance of collaboration among experts to push forward the integration of nonlinear control techniques into various industries. This work highlights theoretical developments in control, and the real-world impact of these systems, showcasing their growing importance in solving complex control problems across multiple fields.[5]

"Como, Giacomo (2025) - Networks, and Communication Systems [Technical Activities]" explores the ongoing advancements within the Networks, and Communication Systems committee. The article reviews key developments in communication protocols, network security, and efficiency, focusing on their critical role in the evolution of global networks. It provides insights into new communication technologies, such as 5G, the Internet of Things (IoT), and cloud computing. The paper discusses challenges like latency, congestion, and scalability, and highlights the committee's role in addressing these issues to shape the future of networking. It is a crucial reflection on how communication technologies are evolving to meet the demands of modern society.[6]

"Pettersen, Kristin Y; Ozay, Necmiye; Joh… (2025) - Historical Women Influencers in Automatic Control [Member Activities]" sheds light on the historical contributions of women in the field of automatic control. This paper highlights the often-overlooked work of female pioneers who have had a lasting impact on control theory, and systems. It discusses their achievements, and how their contributions have shaped the current state of automatic control. The authors advocate for greater diversity in STEM fields, specifically in engineering, to ensure equal representation. The paper emphasizes the significance of recognizing these historical figures to inspire future generations of women in engineering, and technical fields.[7]

"Bernstein, Dennis S (2025) - The Frequency Domain [25 Years Ago]" revisits the foundational work in the frequency domain of control systems that took place 25 years ago. Bernstein's paper provides a retrospective view on the impact of frequency-domain analysis, which has been pivotal in understanding the dynamics of systems, especially regarding stability, and performance. The paper highlights how frequency-domain techniques for system identification, and controller design were developed, and applied. It also discusses how these methods have evolved, and continue to influence modern control systems, robotics, and signal processing, ensuring their relevance in contemporary applications.[8]

"Beck, Carolyn; Johansson, Karl H; Maste… (2025) - Diversity, Outreach, and Development in the CSS [President's Message]" addresses the importance of diversity, and inclusion within the Control Systems Society (CSS). The paper discusses the value of diverse perspectives in fostering innovation within the control systems field. The authors review the society's outreach, and mentorship programs that aim to increase participation from underrepresented groups in control systems research. The message highlights the need for continued support in professional development programs that not only enhance technical expertise but also create a welcoming, and inclusive environment within the field. This message underscores the CSS's commitment to driving progress through diversity.[9]

"Hoang, Minh Long; Carratù, Marco; Paci… (2021) - Noise Attenuation on IMU Measurement For Drone Balance by Sensor Fusion" explains how sensor fusion techniques can be used to improve drone balance by reducing noise in IMU sensor measurements. Drones rely heavily on IMUs for orientation, but sensor noise can cause instability. The authors propose an algorithm that fuses data from accelerometers, gyroscopes, and magnetometers to filter out noise, improving drone performance. The paper compares various filtering techniques, such as Kalman, and complementary filters, to enhance stability during flight. This approach addresses key challenges in drone control systems, particularly in dynamic environments, where precise balance is crucial for safe operation.[10]

"Petrov, Panayot L (2023) - IMU Sensor Fusion with Quaternion Interval-Based Orientation Filters Processed over Smartphone Scanned Data" introduces a novel IMU sensor fusion technique for accurate orientation estimation on smartphones. The paper focuses on quaternion-based filters, which offer a more stable, and efficient representation of 3D rotations compared to traditional Euler angles. Petrov presents an interval-based method that handles uncertainty, and noise in sensor data, enhancing the robustness of orientation estimation. This technique is valuable in applications such as augmented reality (AR), virtual reality (VR), and motion tracking, where precise, and reliable orientation data is essential for user experience, and application accuracy.[11]

"Yoo, Jin-Hyung; Jung, Tae-Uk (2020) - A Study on Output Torque Analysis, and High Efficiency Driving Method of BLDC Motor" examines the performance of Brushless DC (BLDC) motors, specifically focusing on torque generation, and driving efficiency. BLDC

motors are known for their high efficiency, making them ideal for applications such as robotics, and electric vehicles. The paper explores the relationship between motor speed, load, and voltage, and introduces a new method to optimize torque while minimizing energy consumption. Experimental results validate the proposed approach, demonstrating improved motor performance under various operating conditions, which can significantly enhance the energy efficiency of BLDC motor-driven systems.[12]

2.1 Research Gaps

- Limited ESC Control Methods
    - Current ESCs primarily use open-loop control systems
    - Lack of Back EMF integration reduces efficiency and responsiveness
- Market Shortage of Custom Solutions
    - Most available ESCs and IMUs rely on microcontrollers
    - Need for application-specific designs to improve performance
- Underutilized Sensor Fusion Techniques
    - Insufficient exploration of advanced filtering (e.g., Kalman Filter)
    - Potential to enhance accuracy in dynamic operating conditions
- Lack of ESC-IMU Integration
    - Existing IMUs do not incorporate ESC or motor condition data
    - Missed opportunity for comprehensive system optimization

Chapter 3

Project Description

This chapter outlines the overall architecture of the proposed project, and the key steps involved in its development. It explains the function, and significance of each major component, including the ESC control, and IMU interface. The flow of the software is discussed, along with how the system operates, and responds under different runtime conditions.

3.1 Problem Definition

Unmanned Aerial Vehicles (UAVs) require precise motor control, and accurate attitude data for stable flight operations. Traditional Electronic Speed Controllers (ESCs) often rely on microcontroller-based systems, which can introduce latency, limiting real-time control, and responsiveness. Similarly, Inertial Measurement Units (IMUs) used in UAVs must provide highly accurate, and real-time position, and orientation data for smooth maneuvering. The challenge is to develop a system that can handle both precise motor control, and high-speed sensor data processing in a way that improves flight stability, control efficiency, and scalability across different UAV platforms. Additionally, the system needs to ensure reliable real-time communication between the ESC, and IMU for optimized drone performance under varying flight conditions.

3.2 Proposed Solution

The proposed solution for the FPGA-based ESC, and IMU integration project involves using Xilinx VIVADO, and the VIVADO SDK to implement a high-performance Electronic Speed Controller (ESC) for a sensorless BLDC motor. The system will be built around the Zynq Processing System where the ESC control algorithm, including back-EMF zero-crossing detection, and commutation logic, is implemented entirely in C using the Xilinx SDK. The PWM signals required to drive the BLDC motor phases will be generated using AXI Timer or custom logic accessible via memory-mapped I/O, and motor phase switching will be controlled through AXI GPIO connected to external gate driver ICs like the IR2110.

To provide orientation, and motion data, an Inertial Measurement Unit (IMU) such as the MPU6050 will be interfaced via I2C using the XIicPs driver. The real-time accelerometer, and gyroscope data from the IMU will be used to implement closed-loop control strategies, such as maintaining balance or adjusting motor RPM based on tilt or external motion. For back-EMF sensing, an external ADC module like the ADS1115 will be used to measure voltages from the floating motor phase lines. This ADC will also communicate over I2C, and the firmware will monitor zero-crossings in software to time the commutations accurately. GPIO channels will be used to compare the active phase to the sensed back-EMF signal.

The system will also feature UART communication using XUartPs, enabling real-time telemetry, debugging, and configuration. This software-based approach using VIVADO SDK makes the solution modular, easy to debug, and highly portable across FPGA boards. The final result will be a robust, real-time ESC system with sensorless motor control, and IMU-based feedback suitable for drones, robotics, or motion platforms.

Chapter 4

Project Architecture

This chapter presents the architecture of the proposed system along with its corresponding block diagrams. It explains the role, and interaction of each module, illustrating how different components like the ESC logic, IMU interface, and communication channels work together. The diagrams help visualize the system's structure, making it easier to understand the overall data flow, and control mechanisms.

4.1 Block Diagram of Proposed System

In the block diagram of the proposed system, the interaction between the main components is illustrated. It includes the Zynq Processing System, which handles ESC control logic, IMU communication, and data processing. The PWM generation unit controls the gate drivers connected to the BLDC motor, while the ADC module reads back-EMF signals for sensorless commutation. The IMU is interfaced via I2C to provide motion data, and UART is used for telemetry, and debugging. The diagram shows how these blocks communicate to enable real-time, closed-loop motor control.

4.1.1 Architecture of ESC

The provided image outlines a feedback system for Back EMF detection in a Brushless DC (BLDC) motor setup. It includes several key components: the XADC IP (Xilinx Analog-to-Digital Converter Intellectual Property) for signal conversion, the ZYNO PS (likely a Zynq Processing System) for processing, a MOSFET-based motor driver to control the BLDC motor, and a PWM (Pulse Width Modulation) detector for signal analysis. The flight controller manages overall system operations, while the power supply ensures stable energy distribution. Together, these elements form a cohesive system for monitoring and controlling the BLDC motor using Back EMF feedback.

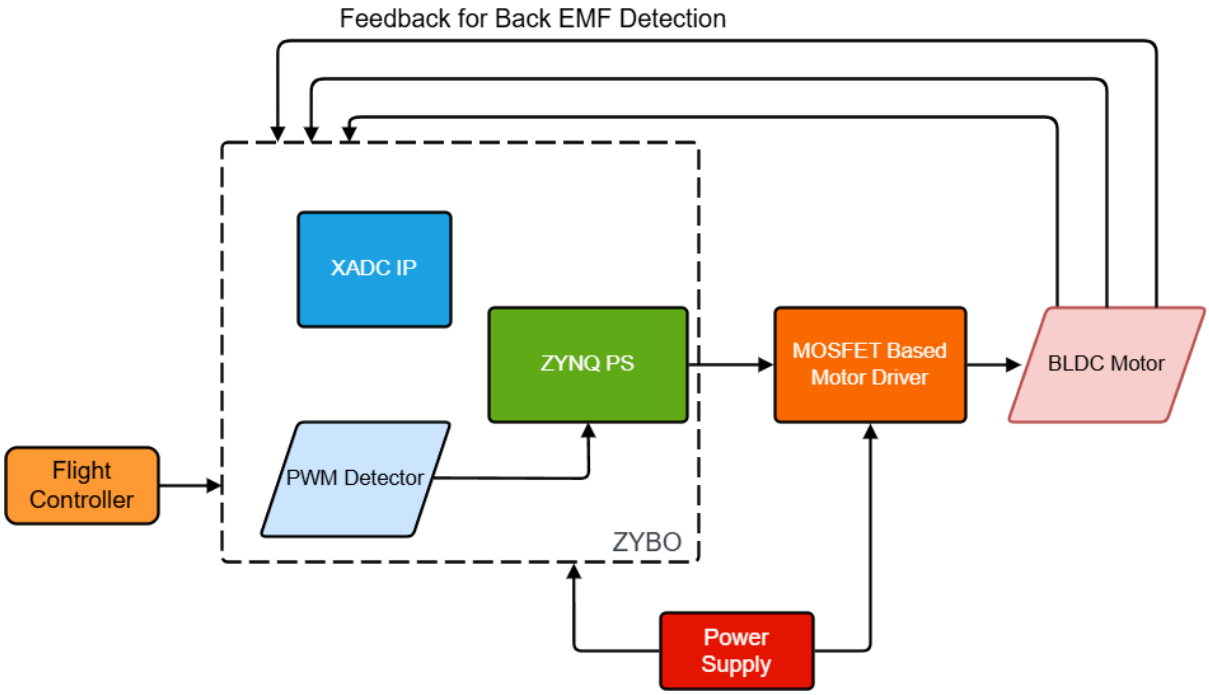

Fig 1 Architecture of ESC

1. **Flight Controller:** The Flight Controller serves as the main interface between the user, and the ESC. It generates Pulse Width Modulation (PWM) signals, which encode speed, and control instructions based on input from sensors or remote comm, ands. These signals need to be decoded before being processed by the ESC system.
2. **PWM Detector:** The PWM Detector is responsible for extracting control information from the PWM signal received from the flight controller. It interprets the duty cycle, and converts it into a digital signal that can be further processed by the ZYNQ Processing System (PS). This ensures that the control comm, ands are accurately translated into motor actions.
3. **ZYNQ PS:** The ZYNQ PS acts as the central processing unit of the ESC. It processes input data from the PWM Detector, and the XADC IP (Xilinx Analog-to-Digital Converter), making real-time decisions to regulate motor speed, and torque. The XADC IP is an essential component that converts analog signals—such as back-EMF (electromotive force) or current measurements into digital form, allowing precise monitoring, and feedback control. This enables sensor less motor control, where the ESC determines rotor position without using additional sensors.
4. **MOSFET Based Motor Driver:** Once the control logic determines the appropriate action, the MOSFET-Based Motor Driver is activated. This driver consists of a full-bridge or half-bridge MOSFET circuit that rapidly switches the motor phases on, and off, allowing smooth, and efficient power delivery to the BLDC motor. The MOSFETs are controlled

using high-frequency signals to ensure accurate commutation of the motor phases, optimizing performance, and efficiency.

5. **BLDC Motor:** The BLDC Motor is the final component in the system, which converts electrical energy into mechanical motion. The precise switching of the MOSFETs ensures efficient motor operation, minimizing losses, and providing smooth acceleration, and speed control. The back-EMF generated by the motor is fed back to the XADC IP, allowing real-time monitoring, and adjustments to maintain stable performance.
6. **Power Supply:** Finally, the Power Supply provides the necessary voltage, and current to operate the entire system, including the ZYBO FPGA board, motor driver circuit, and peripherals. The power source must be capable of handling high current surges required by the motor while maintaining stable operation of the digital control system.

4.1.2 Architecture of IMU

The image depicts a sensor data acquisition and processing system centered around the ZYBO (a Xilinx Zynq-based development board). It includes multiple sensors—MPU6050 (accelerometer and gyroscope), BMP280 (barometric pressure sensor), and HMC5883L (magnetometer)—all communicating via I²C (SDA/SCL lines). An I²C IP core facilitates data transfer, enabling register-wise data acquisition for sensor readings. The Kalman Filter processes raw data to refine measurements, producing outputs such as rotational acceleration (X, Y, Z) and translational orientation (roll, pitch, yaw). Processed data is transmitted via UART (TX/RX) for further use. The power supply ensures stable operation, making this a complete system for motion sensing, environmental monitoring, and orientation tracking.

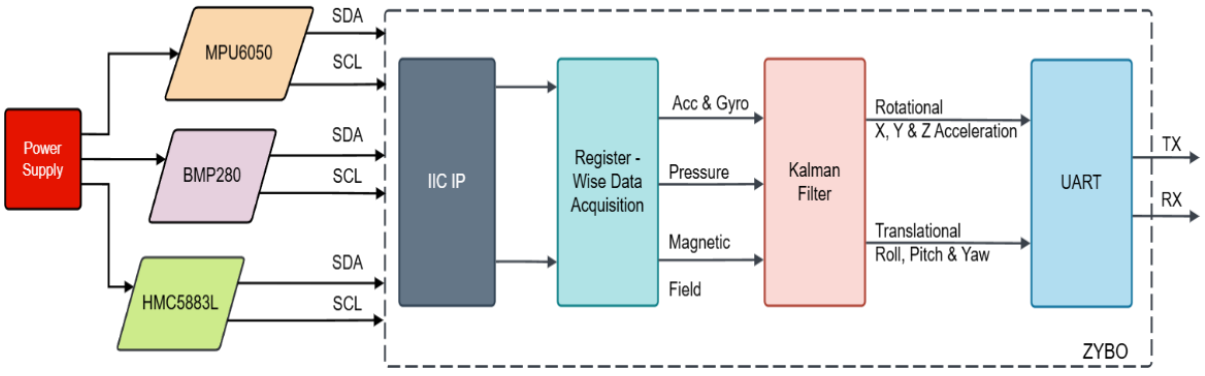

Fig 2 Architecture of IMU

1. **Power Supply:** The Power Supply is responsible for providing stable voltage, and current to the IMU sensors, and processing units. It ensures the sensors operate reliably, avoiding data corruption due to power fluctuations.
2. **Sensors:** The IMU system incorporates three key sensors that work together to provide comprehensive motion, and environmental data. The MPU6050 is a 6-axis inertial measurement unit that integrates a 3-axis accelerometer, and a 3-axis gyroscope. The accelerometer measures linear acceleration along the X, Y, and Z axes, while the gyroscope detects rotational motion, allowing for precise tracking of orientation, and movement. The BMP280 is a barometric pressure sensor designed to measure atmospheric pressure, and altitude with high accuracy. By analyzing pressure variations, it enables altitude estimation, which is particularly useful in drone navigation, and environmental monitoring applications. The HMC5883L is a 3-axis magnetometer that detects the Earth's magnetic field, enabling precise heading determination. When combined with accelerometer, and gyroscope data, it provides a stable, and drift-free orientation reference, crucial for navigation systems, robotics, and flight stabilization. These sensors collectively offer a robust solution for motion tracking, and environmental awareness.
3. **I2C Communication:** These sensors communicate through the IIC (I2C) IP, which acts as a bridge between the sensors, and the processing system. The IIC IP (Inter-Integrated Circuit Intellectual Property) module enables efficient data transfer by reading values from each sensor's internal registers.
4. **Register-Wise Data Acquisition:** Once the data is collected, it is sent to the Register-Wise Data Acquisition module, which organizes, and stores the sensor data in specific registers for further processing. This step ensures that the data remains structured, and accessible for real-time computation.
5. **Kalman Filter:** To improve accuracy, and reduce noise, the system implements a Kalman Filter. The Kalman Filter is an advanced algorithm that fuses data from the accelerometer, gyroscope, and magnetometer, filtering out noise, and compensating for drift errors. This results in highly accurate orientation, and motion estimation, which is crucial for applications such as robotic navigation, and drone stabilization.
6. **UART Communication Module:** Finally, the processed data is sent to the UART (Universal Asynchronous Receiver-Transmitter) module, which enables serial communication with external devices. This allows the IMU data to be transmitted to a microcontroller, computer, or flight controller for further use in real-time applications.

4.2 Component Description

4.2.1 Hardware

The system integrates multiple hardware components for motion control and sensing. The ZYBO (a Xilinx Zynq-based FPGA board) serves as the central processing unit, coordinating sensor inputs and motor control. Key sensors include the MPU6050 (6-axis accelerometer and gyroscope) for motion tracking, the BMP280 (barometric pressure sensor) for altitude measurement, and the HMC5883L (magnetometer) for compass-based orientation. A BLDC motor is driven by an IR2101 MOSFET gate driver and IRF3205 power MOSFETs, which regulate motor speed and direction using PWM signals. Power is supplied by an 11.1V 2200mAh 40/80C 3S LiPo Battery, providing high-current output for motor operation and system stability. Together, these components form a robust setup for applications such as drones, robotics, or precision motion control, combining real-time sensor feedback with efficient motor actuation.

4.2.1.1 ZYBO Board

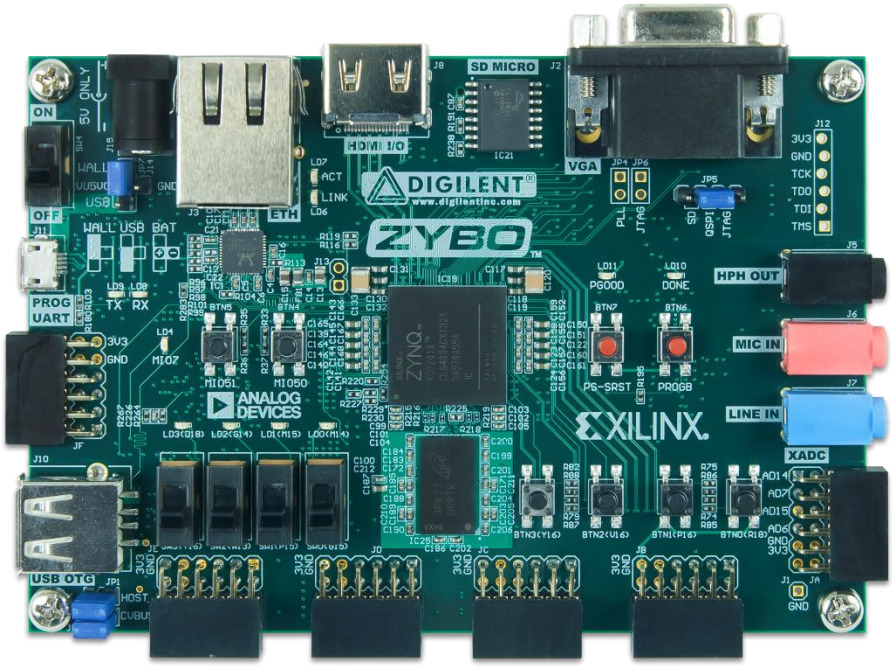

Fig 3 ZYBO Board *[13]*

The Zybo Legacy Board is a versatile FPGA development board based on the Xilinx Zynq-7000 SoC, integrating a dual-core ARM Cortex-A9 processor with programmable logic. This combination allows for a powerful balance between hardware acceleration, and software programmability, making it ideal for embedded systems, digital signal processing, and custom

hardware design. The board features 512MB DDR3 RAM, providing sufficient memory for running complex applications, along with 16MB Quad-SPI Flash for non-volatile storage. Multiple connectivity options include USB OTG, which supports host, and device modes, USB UART for serial communication, Gigabit Ethernet for high-speed networking, and a microSD card slot for external storage, and booting Linux-based systems. For multimedia applications, the Zybo supports HDMI, and VGA output, enabling the development of video processing projects, alongside stereo audio input, and output, which allows for audio signal processing, and multimedia interfacing. Additionally, the board offers GPIOs, push buttons, and switches** for user interaction, as well as PWM, SPI, I2C, and UART interfaces for connecting peripherals, and communication with other devices. Expansion capabilities include two Pmod ports, which allow for the integration of additional modules such as sensors, communication interfaces, and custom hardware extensions. The XADC module provides support for analog signal processing, making the Zybo suitable for data acquisition, and sensor interfacing. The Zybo is widely used in applications such as FPGA-based control systems, embedded Linux development, AI/ML acceleration, robotics, and sensor-based automation. It has been a popular choice for students, researchers, and developers due to its balance of performance, cost, and flexibility. While it has been succeeded by newer models like the Zybo Z7, the Zybo Legacy Board continues to be a reliable platform for FPGA prototyping, hardware experimentation, and educational purposes in digital design, and embedded systems. [13]

4.2.1.2 MPU6050

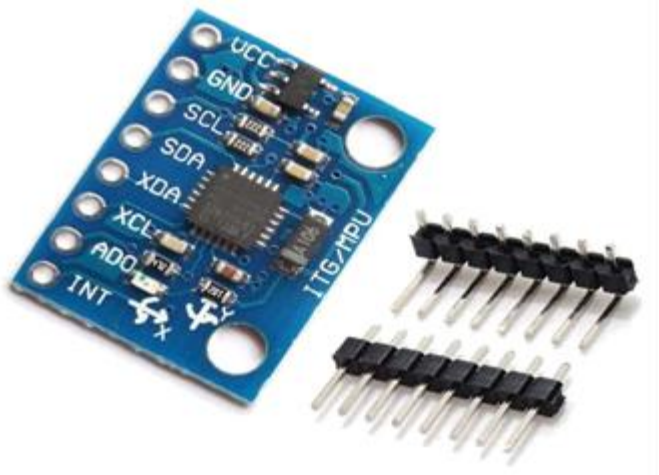

Fig 4 MPU6050 Gyroscope and Accelerometer *[14]*

The MPU6050 is a versatile 6-axis motion tracking device that combines a 3-axis accelerometer, and a 3-axis gyroscope into a single compact package. Designed for motion-

sensing applications such as drones, robotics, and smartphones, it communicates via the I2C protocol, and operates within a voltage range of 2.375V to 3.46V. The accelerometer measures linear acceleration along the X, Y, and Z axes, while the gyroscope detects angular velocity around the same axes, making it ideal for monitoring both orientation, and rotational movement. It features 16-bit analog-to-digital converters (ADCs) for high-resolution data acquisition. Additionally, the integrated Digital Motion Processor (DMP) can offload sensor fusion algorithms, reducing the computational burden on external processors. The MPU6050 also includes a temperature sensor for compensating sensor drift, ensuring more reliable data. Its low power consumption makes it suitable for battery-powered devices, and its real-time motion data capabilities are widely used in control systems that require precision, and stability. [14]

4.2.1.3 BMP280

Fig 5 BMP280 Pressure Sensor *[15]*

The BMP280 is a high-precision, low-power barometric pressure sensor designed for applications such as altitude measurement, weather monitoring, and GPS enhancement. It operates over a wide voltage range of 1.71V to 3.6V, and communicates through both I2C, and SPI interfaces. The sensor measures absolute pressure, which can be used to estimate altitude with an accuracy of ±1 meter, and also integrates a temperature sensor for environmental monitoring. The BMP280 features a 24-bit analog-to-digital converter (ADC), ensuring high-resolution pressure, and temperature data. Its low power consumption makes it ideal for battery-operated devices, and it is often used in mobile devices, wearables, and UAVs for accurate altitude tracking, and weather-related data. The BMP280's small form factor, and

robust performance make it a popular choice for applications requiring precise atmospheric pressure readings. [15]

4.2.1.4 HMC5883L

***Fig 6 HMC5883L Magnetometer** [16]*

The HMC5883L is a three-axis digital magnetometer developed by Honeywell, widely used for electronic compasses, navigation systems, and motion tracking. It operates via I2C communication, providing raw magnetic field data along the X, Y, and Z axes. With a configurable measurement range of ±1.3 to ±8.1 Gauss and a 12-bit ADC resolution, it provides precise magnetic field readings while maintaining low power consumption (operating voltage 2.16V to 3.6V). Built on Anisotropic Magneto-Resistive (AMR) technology, the sensor detects minute changes in magnetic fields with high sensitivity and accuracy, making it ideal for applications such as navigation systems, vehicle detection, augmented reality, and gaming controllers. Its compact design, high resolution, and simple microcontroller interfacing have made it a popular choice for embedded systems, drones, and robotics. However, the HMC5883L requires manual calibration to compensate for distortions caused by nearby ferromagnetic materials, and it lacks built-in tilt compensation, meaning additional sensors (like an accelerometer) may be needed for full orientation sensing. While newer alternatives such as the QMC5883L offer improved features like automatic calibration and higher refresh rates, the HMC5883L remains widely used in cost-sensitive applications due to its proven reliability and ease of integration. Its balance of performance, affordability, and simplicity ensures its continued relevance in DIY electronics, academic projects, and industrial sensing systems. [16]

4.2.1.5 BLDC Motor

Fig 7 BLDC Motor *[17]*

The A2212/13T 1000KV BLDC motor is a popular brushless DC motor designed primarily for use in quadcopters, drones, and RC aircraft. It is a three-phase motor with a KV rating of 1000, meaning it rotates at 1000 RPM per volt applied without load. Designed for small to medium UAVs (drones), it operates efficiently within a voltage range of 7.4V to 12.6V (compatible with 2S to 3S LiPo batteries) and generates sufficient thrust for agile flight performance. The motor features a 3.17mm shaft diameter and a lightweight yet durable aluminum casing (weighing approximately 50g), ensuring structural integrity without compromising weight—a critical factor for flight stability and maneuverability. Optimized for 8 to 10-inch propellers, this motor draws 10A to 20A of current, depending on propeller size and aerodynamic load. Its brushless design eliminates friction-based wear, enhancing longevity and reducing maintenance compared to brushed motors. With high torque output and smooth power delivery, this motor is ideal for UAVs, robotics, and other applications demanding reliable, efficient propulsion. The combination of lightweight construction, robust materials, and consistent performance makes it a preferred choice for hobbyists and professionals alike, particularly in scenarios where precision control and endurance are paramount. The BLDC motor's advanced design also incorporates high-quality bearings and precision-balanced rotors, ensuring minimal vibration and noise during operation—key factors for UAV applications where stability and smooth performance are critical. Its efficient thermal management allows sustained high-speed operation without overheating, even under demanding flight conditions. The motor's winding configuration and magnet strength are optimized to deliver rapid throttle response, making it well-suited for dynamic maneuvers in racing drones or precise hovering in aerial photography platforms. [17]

4.2.1.6 IR2101 High, and Low Side Driver IC

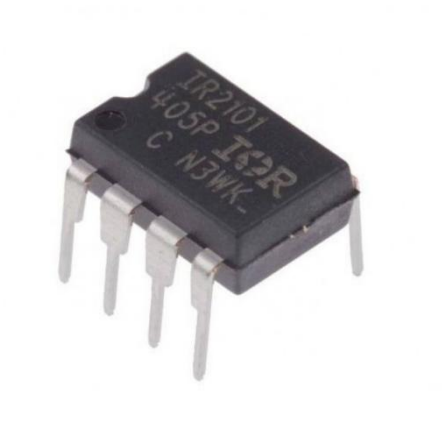

Fig 8 IR2101 High, and Low Side Driver IC *[18]*

The IR2101 is a high-voltage, high-speed half-bridge gate driver designed for driving MOSFETs, and IGBTs in motor control, and power conversion applications. It operates with a supply voltage of up to 600V, and features independent high-side, and low-side outputs with fast switching capability. The device uses a bootstrap circuit for the high-side drive, and includes built-in undervoltage protection. With low power consumption, and a compact design, it is widely used in inverters, motor drivers, and switching power supplies. Proper dead-time management is necessary to prevent shoot-through currents in bridge circuits. [18]

4.2.1.7 IRF3205 MOSFET

Fig 9 IRF3205 MOSFET *[19]*

The IRF3205 is a high-power N-channel MOSFET designed for applications requiring efficient switching, and handling of high current loads. It is commonly used in motor controllers, power supplies, and battery-powered systems due to its low on-resistance, and high current-handling capability. The IRF3205 operates with a drain-to-source voltage (V_{DS}) of up to 55V, and can

handle continuous currents up to 110A, making it suitable for high-power applications. The IRF3205 is housed in a TO-220 package, offering good thermal dissipation, and making it easy to mount on heat sinks for enhanced cooling in high-power operations. This MOSFET is widely used in ESCs for BLDC motors, automotive electronics, and various power switching circuits where low heat generation, and high efficiency are critical. [19]

4.2.1.8 11.1V 2200mAh 40/80C 3S LiPo Battery

Fig 10 11.1V 2200mAh 40/80C 3S LiPo Battery *[20]*

The 11.1V 2200mAh 40C/80C 3S LiPo battery is a high-performance lithium polymer battery commonly used in RC aircraft, drones, and other high-power applications. It consists of three cells (3S) connected in series, providing a nominal voltage of 11.1V. The battery's capacity is 2200mAh, meaning it can deliver 2200mA for one hour of continuous use, or higher currents for shorter durations. The "40C/80C" rating indicates its discharge capabilities. The 40C continuous rating means the battery can discharge at 40 times its capacity, delivering up to 88A (40 × 2.2A) continuously. The 80C burst rating allows it to discharge at up to 80 times its capacity (176A) for short bursts, making it ideal for high-power dem, ands like rapid acceleration or sudden maneuvering in UAVs or RC vehicles. This battery type offers a good balance between weight, power, and capacity, making it a popular choice for small to medium-sized drones, and RC models. Its lithium polymer chemistry ensures a high energy density, providing longer flight times with relatively low weight. Proper care, such as balancing the cells during charging, and avoiding over-discharge, is essential for maintaining its longevity, and safety. [20]

4.2.2 Software

The software implementation for this system will be discussed in detail, covering the tools and frameworks used for development, configuration, and real-time operation. This includes Xilinx Vivado for FPGA programming and hardware-software co-design, embedded C/C++ for microcontroller firmware, and any additional software utilities for sensor calibration, motor control algorithms, and communication protocols. The integration of these software components ensures seamless interaction between the hardware modules, enabling efficient data processing and system.

4.2.2.1 Xilinx VIVADO

Fig 11 Xilinix VIVADO [21]

Xilinx VIVADO is a comprehensive suite of software tools designed for the development, simulation, and implementation of digital circuits on Xilinx FPGAs, and SoCs (System-on-Chips). It offers an integrated environment for hardware design, providing key features like synthesis, analysis, verification, and debugging within a single platform. VIVADO supports both HDL (Hardware Description Language) designs, such as Verilog, and VHDL, and graphical design flows with IP (Intellectual Property) integration, and block diagram creation. It includes high-level synthesis (HLS) to convert C, C++, or SystemC code into RTL, streamlining the process of implementing complex designs. With its design suite, engineers can move seamlessly from specification to hardware debugging, including logic synthesis, place-, and-route, and bitstream generation. The IP Integrator feature enables easy system design by integrating pre-built IP cores through a drag-, and-drop interface. [21]

Chapter 5

Implementation

This chapter covers the implementation of an Electronic Speed Controller (ESC), and Inertial Measurement Unit (IMU). The process begins with hardware setup, followed by defining the control algorithms in VIVADO, and SDK. For the ESC, the BLDC motors are connected to the FPGA, with the correct pin configuration established in VIVADO. Calibration of the MPU6050, and BMP280 sensors is done via SDK, with the sensor data subsequently filtered using a Kalman filter. The detailed procedure is outlined below.

5.1 Working of the Project

5.1.1 Electronic Speed Controller (ESC)

1. PWM Signal Reading: The ESC detects the PWM signals generated by the flight controller, which dictate the desired motor speed.
2. PWM to Duty Cycle Conversion: The ESC converts the PWM signals into a corresponding duty cycle. This duty cycle determines the duration the motor should be powered on versus off, effectively controlling the motor's speed.
3. Generate PWM Signal for Motor Driver: Based on the calculated duty cycle, the ESC generates a PWM signal to drive the motor driver (H-Bridge), which controls the power delivered to the motor.
4. Feedback, and Correction: To maintain the desired motor speed, the ESC continually senses back EMF (Electromotive Force) from the motor. This feedback is crucial for estimating the actual motor speed.
5. Speed Comparison: The ESC compares the measured motor speed with the desired speed. If the speeds match, the system maintains the current PWM signal. If there is a discrepancy, the ESC adjusts the PWM signal to correct the motor speed.
6. Utilizing XADC IP: The XADC (Analog-to-Digital Converter) IP within the FPGA facilitates the acquisition of analog signals, such as voltage measurements from the motor, enhancing the ESC's ability to monitor, and control motor performance effectively.
7. Control Loop: This feedback loop ensures that the motor operates within the desired parameters, optimizing performance, and stability. The process repeats continuously, allowing for real-time adjustments based on flight conditions.

5.1.2 Inertial Measure Unit (IMU)

1. System Initialization (FPGA Powered ON)
2. The ZYNQ Processing System (PS), and its peripherals, including I2C, and UART interfaces, are initialized to enable communication with sensors.
3. The ZYNQ program is loaded, setting up the necessary logic for data acquisition, and processing.
4. I2C, and UART IPs are configured to establish a connection with external sensors, and facilitate data transmission.
5. The I2C peripherals are initialized, and the MPU6050 (accelerometer, and gyroscope), BMP280 (barometric pressure sensor), and HMC5883L (magnetometer) are configured for operation.
6. Sensor data is read, including acceleration, and gyroscope data from MPU6050, pressure readings from BMP280, and magnetic field measurements from HMC5883L.
7. The collected sensor data is processed using a Kalman filter to compute roll, pitch, and yaw, reducing noise, and improving accuracy.
8. The processed data is transmitted to external systems via UART, and may also be output to GPIO pins for further use.
9. The system checks if it needs to continue or exit. If not exiting, the loop repeats, continuously acquiring, and processing data.
10. Once the sensors are configured, data is acquired from both MPU6050 (acceleration, and gyroscope data), and BMP280 (pressure/altitude data). This is done by reading specific registers of the sensors through IIC.

If an exit condition is met, the process stops, ending the system's operation.

5.2 Hardware

1. ZYBO Board: The ZYBO board is used for ESC control, and IMU processing, leveraging its FPGA, and ARM Cortex-A9 processor. It generates PWM signals for BLDC motor control, processes back-EMF feedback via XADC, and interfaces with MPU6050, BMP280, and HMC5883L over I2C. A Kalman filter refines sensor data for accurate orientation estimation, while UART transmits processed results. Its high-speed processing makes it ideal for real-time motor, and sensor control.

2. MPU6050: Connect the MPU6050 (accelerometer, and gyroscope) via I2C to the FPGA board. Use Verilog or VHDL code to interface with the sensor, reading motion, and orientation data.
3. BMP280: Connect the BMP280 (pressure, and temperature sensor) via I2C to the FPGA board. Capture temperature, pressure, and altitude data by writing an FPGA interface.
4. HMC5883L: The HMC5883L magnetometer is connected via I2C to provide heading direction by measuring the Earth's magnetic field. This data, combined with the MPU6050, and BMP280, enhances orientation tracking, and navigation accuracy.
5. BLDC Motor: A Brushless DC (BLDC) motor operates using an electronic commutation system, which replaces the mechanical brushes and commutators found in traditional brushed motors. This design eliminates friction-based wear, significantly improving efficiency, reliability, and lifespan. BLDC motors are capable of high-speed operation, precise torque control, and rapid acceleration, making them ideal for applications demanding dynamic performance and energy efficiency, such as drones, robotics, industrial automation, and electric vehicles.
6. IR2101: The IR2101 is a high-voltage, high-speed gate driver designed for driving N-channel MOSFETs in half-bridge configurations. It features independent high-side, and low-side outputs, making it ideal for motor control, power inverters, and switching applications. Its built-in dead-time control ensures safe operation, preventing shoot-through currents in MOSFET-based driver circuits.
7. IRF3205: The IRF3205 is an N-channel MOSFET used for switching, and amplification in high-current applications. Its low on-resistance makes it suitable for motor control, and power supply circuits.
8. 11.1V 2200mAh 40/80C 3S LiPo Battery: This 3-cell (3S) Lithium Polymer (LiPo) battery delivers a nominal voltage of 11.1V (with a full charge voltage of 12.6V), combined with a 2200mAh (2.2Ah) capacity, providing a robust energy supply for power-hungry applications. Its high discharge capabilities—40C continuous (88A) and 80C burst (176A)—make it exceptionally well-suited for demanding, high-performance systems like racing drones, industrial robotics, and RC vehicles, where rapid power delivery and reliability are critical.

5.3 Electronic Speed Controller (ESC) Flow

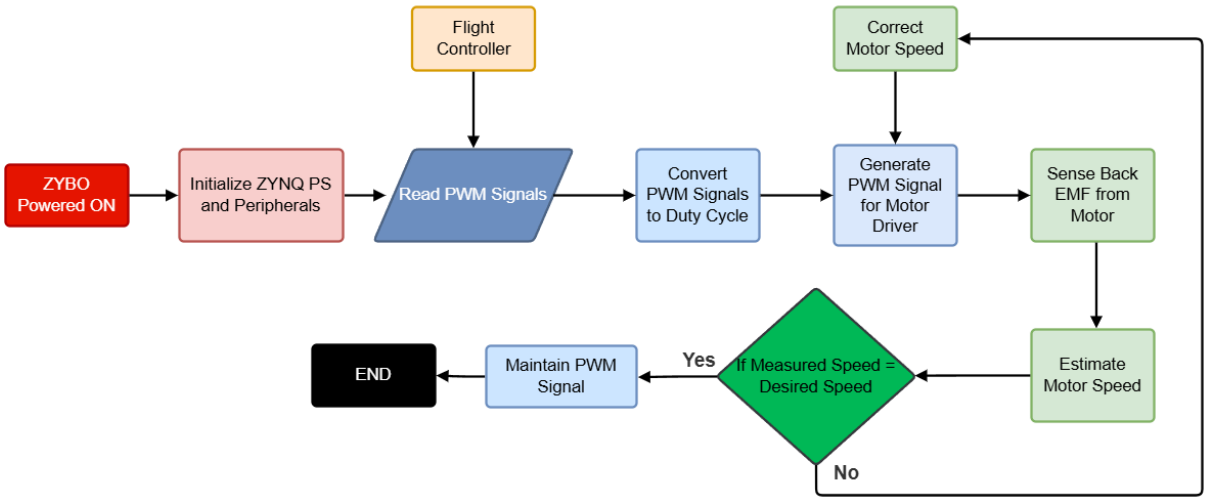

Fig 12 Electronic Speed Controller Flow

1. **Zybo Powered ON**: The system begins when the Zybo board is powered on, initializing the ESC control process.
2. **Initialize ZYNQ PS, and Peripherals**: The ZYNQ Processing System (PS), and its connected peripherals (such as I2C, PWM, and ADC modules) are initialized to establish communication with the sensors, and motor driver.
3. **Read PWM Signals**: The ESC reads PWM input signals from the Flight Controller, which determines the desired motor speed.
4. **Convert PWM Signals to Duty Cycle**: The received PWM signal is converted into a corresponding duty cycle, which determines the power delivered to the motor.
5. **Generate PWM Signal for Motor Driver:** Based on the computed duty cycle, a new PWM signal is generated, and sent to the MOSFET-based motor driver, controlling the power applied to the BLDC motor.
6. **Sense Back-EMF from Motor**: The system measures the back-electromotive force (back-EMF) generated by the motor, which provides real-time feedback about its speed.
7. **Estimate Motor Speed**: Using the back-EMF data, the actual motor speed is estimated, and compared with the desired speed.
8. **Speed Comparison**: The measured speed is checked against the desired speed:
    - If the speeds match, the system maintains the current PWM signal, ensuring stable motor operation.

- If the speeds do not match, the system applies corrections by adjusting the PWM signal to achieve the desired speed.

9. **Correct Motor Speed**: If necessary, the system fine-tunes the motor control parameters to achieve the correct speed, completing the feedback loop.
10. **Maintain PWM Signal / End**: Once the speed is stabilized, the ESC continuously maintains the PWM output, ensuring the motor runs at the required speed until new control signals are received.

5.4 Inertial Measurement Unit (IMU) SDK Flow

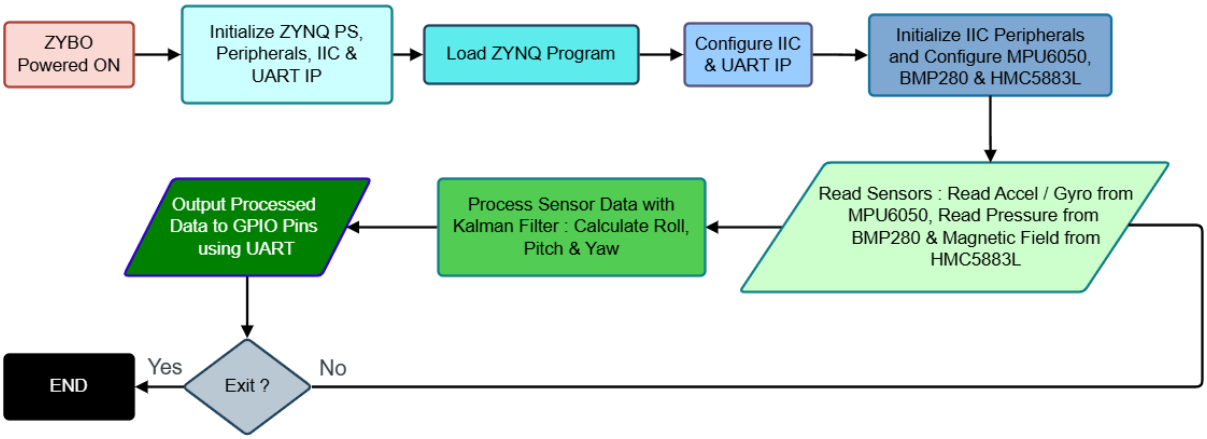

Fig 13 Inertial Measurement Unit Flow

1. **Zybo Powered ON**: The process begins when the Zybo board is powered on, preparing the system for initialization.
2. **Initialize ZYNQ PS, Peripherals, IIC & UART IP**: The ZYNQ Processing System (PS), and essential peripherals like I2C (Inter-Integrated Circuit), and UART (Universal Asynchronous Receiver-Transmitter) are initialized for communication with sensors, and external systems.
3. **Load ZYNQ Program**: The FPGA loads the pre-configured ZYNQ program that will control the IMU data acquisition, and processing.
4. **Configure IIC & UART IP**: The IIC interface is configured to enable communication with the connected sensors, while the UART is set up for data transmission.
5. **Initialize IIC Peripherals, and Configure Sensors**: The MPU6050 (accelerometer & gyroscope), BMP280 (barometric pressure sensor), and HMC5883L (magnetometer) are initialized, and configured for data acquisition.
6. **Read Sensor Data** – Sensor readings are collected:
    - **MPU6050** provides acceleration, and gyroscope data.

- **BMP280** records atmospheric pressure for altitude estimation.
- **HMC5883L** measures the Earth's magnetic field to determine heading.

7. **Process Sensor Data with Kalman Filter**: The collected sensor data is processed using a Kalman filter, which fuses information from multiple sensors to accurately compute roll, pitch, and yaw angles, reducing noise, and improving stability.
8. **Output Processed Data to GPIO Pins using UART**: The final processed sensor data is transmitted to an external system via UART, and may also be sent to GPIO pins for further use.
9. **Exit Check**: The system checks whether it should continue processing or exit. If No, the loop repeats, continuously acquiring, and processing sensor data. If yes, the program ends.

Chapter 6

Results, and Conclusion

6.1 Environmental Setup

Begin by installing Xilinx Vivado and SDK. For the IMU system, connect the MPU6050 (accelerometer/gyroscope), BMP280 (pressure sensor), and HMC5883L (magnetometer) to the FPGA via I²C, ensuring stable power and ground. In Vivado SDK, initialize I²C and UART for sensor data acquisition and transmission. Implement a Kalman filter for sensor fusion, computing roll, pitch, and yaw, then transmit processed data via UART for external use. For BLDC motor control, configure the FPGA to interface with the ESC. Connect motor phases to the MOSFET driver (IR2101 + IRF3205) and route back-EMF signals to the XADC for sensorless speed estimation. Implement PWM generation, zero-crossing detection, and phase commutation in the FPGA. Test the system by validating motor response, feedback loops, and stability under varying loads. This setup ensures real-time sensor processing and precise motor control, critical for UAV and robotics applications.

Hardware Requirements

ZYBO Board: For implementing the control algorithms of ESC, and IMU.
MOSFET Gate Driver Circuit: A circuit that amplifies control signals from the ZYBO board to drive the MOSFETs efficiently, ensuring proper switching, and minimizing power losses.
MOSFET Based Motor Driver: A high-power switching circuit using MOSFETs to control the BLDC motor by regulating power delivery based on PWM signals from the ESC.
Motors: Brushless DC motors (BLDC) that are controlled by the ESC.
MPU6050: For capturing accelerometer, and gyroscope data.
BMP280: For barometric pressure, and altitude measurements.
HMC5883L: For magnetometer readings, enabling accurate heading estimation.
Power Supply: Provides appropriate power for the FPGA, IMU sensors, and BLDC Motors.

6.2 Results

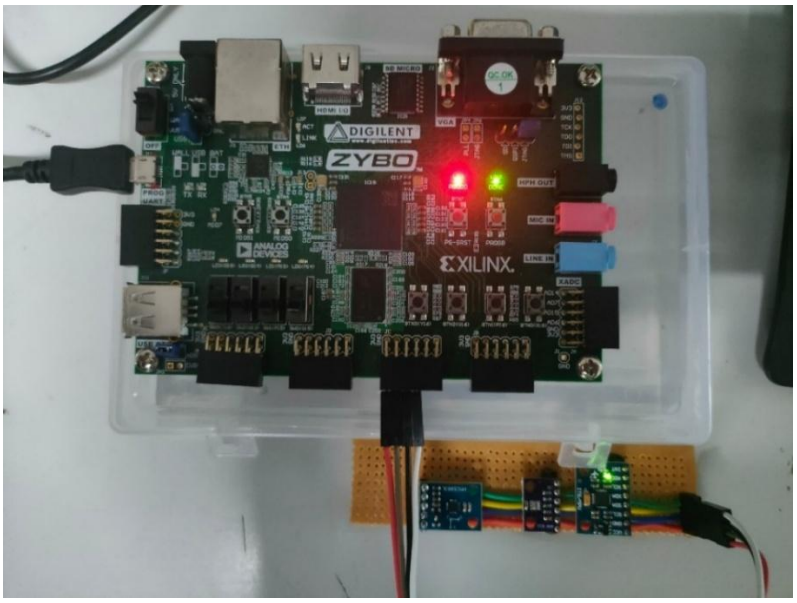

Fig 14 IMU Hardware Implementation

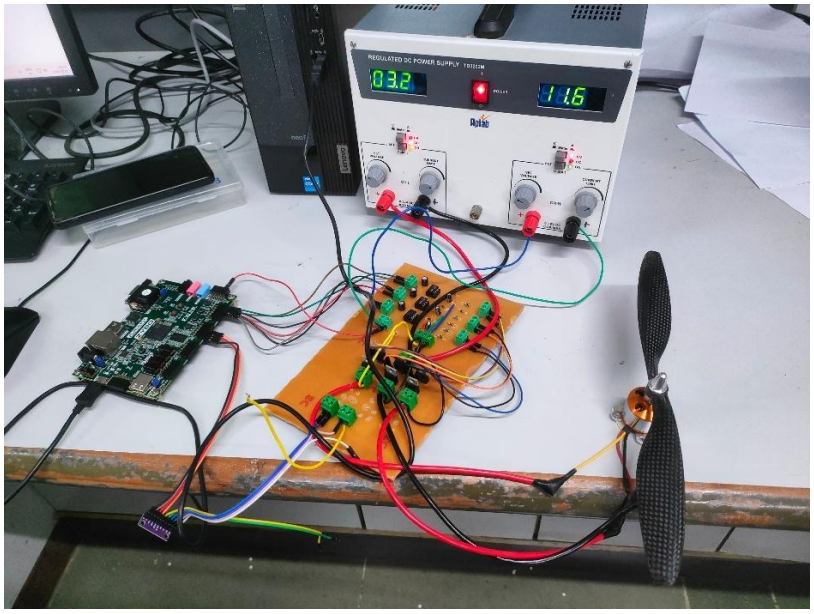

Fig 15 ESC Hardware Implementation

Fig 14 and 15 present the hardware implementation details of the IMU (Inertial Measurement Unit) and ESC (Electronic Speed Controller) systems respectively.

Fig 14 focuses on the IMU subsystem, illustrating the FPGA-based hardware architecture for interfacing with the MPU6050 (accelerometer/gyroscope), BMP280 (pressure sensor), and HMC5883L (magnetometer) via I²C communication. The design incorporates the sensor fusion algorithm (Kalman filter) implemented in hardware logic to compute the roll, pitch, and yaw

angles in real-time. Key components like the I²C controller, data processing pipelines, and UART interface for data output are clearly depicted, demonstrating an optimized architecture that achieves low-latency performance within the FPGA's resource constraints.

Figure 15 showcases both the FPGA logic implementation and the custom-designed ESC PCB. The FPGA portion details the PWM generation module, back-EMF sensing through XADC, and the commutation control logic for sensorless BLDC motor control. The accompanying ESC PCB features the power stage with IRF3205 MOSFETs, IR2101 gate drivers, and supporting circuitry for robust motor driving. The board layout emphasizes proper power routing, noise isolation, and thermal management to ensure reliable high-current operation.

Together, these figures highlight a tightly integrated hardware solution that combines real-time sensor processing with high-performance motor control, all while maintaining efficient FPGA resource usage as shown in the utilization table. The modular yet optimized design makes this implementation suitable for demanding applications like UAV flight control systems.

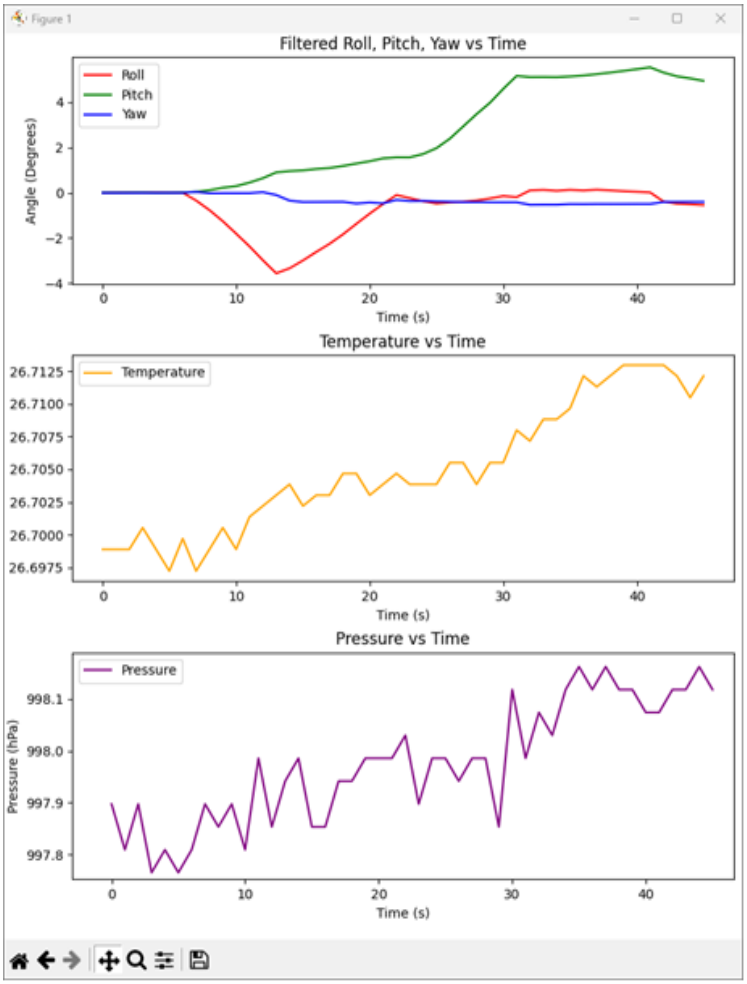

Fig 16 Simulated Kalman Filter

For the IMU data, sensor values, including accelerometer, and gyroscope data, were received via the SDK, and processed in real-time. A Kalman filter was applied to reduce noise, ensuring accurate roll, pitch, and yaw measurements. The filtered results show the roll angle dipping below zero, and returning to near its initial value, while the pitch angle increases steadily to around 4 degrees over 40 seconds. The yaw angle remained stable near zero. Additionally, environmental data such as temperature, and pressure were tracked. Temperature rose slightly from 26.6975°C to 26.7125°C, while pressure fluctuated between 997.8 hPa, and 998.1 hPa, indicating small environmental changes.

- **Filtered Roll, Pitch, Yaw vs Time (Top Plot):** This plot shows the angles of roll (in red), pitch (in green), and yaw (in blue) as they change over time. The roll angle starts near zero, dips below, and then returns close to its initial value. The pitch angle begins near zero, increases steadily after around 10 seconds, and reaches approximately 4 degrees by 40 seconds. The yaw angle remains mostly steady, with minimal fluctuations around the zero mark throughout the time period. This data comes from an IMU (Inertial Measurement Unit), likely the MPU6050, and represents the system's orientation in 3D space.
- **Temperature vs Time (Middle Plot):** The middle plot shows the temperature measured over time, with the temperature increasing gradually from approximately 26.6975°C to 26.7125°C over a period of about 45 seconds. The data shows small fluctuations but generally trends upward, indicating a slow rise in temperature over time.
- **Pressure vs Time (Bottom Plot):** The bottom plot illustrates pressure measurements over time, with values fluctuating between 997.8 hPa, and 998.1 hPa. The pressure data shows some sharp variations but generally trends upward with small peaks, and valleys, indicating changing environmental conditions or sensor responses.

Site Type	Used	Fixed	Available	Util%
Slice LUTs	1459	0	17600	8.29
LUT as Logic	1397	0	17600	7.94
LUT as Memory	62	0	6000	1.03
LUT as Distributed RAM	0	0		
LUT as Shift Register	62	0		
Slice Registers	1473	0	35200	4.18
Register as Flip Flop	1473	0	35200	4.18
Register as Latch	0	0	35200	0.00
F7 Muxes	0	0	8800	0.00
F8 Muxes	0	0	4400	0.00

Fig 17 Hardware Utilization Report

The FPGA resource utilization results demonstrate efficient implementation of both the ESC and IMU systems on the Zynq-7000 platform. The design utilizes 1,397 Slice LUTs (7.94% of available 17,600) and 1,473 Slice Registers (4.18% of 35,200), showing balanced logic and storage allocation. A modest 62 LUTs (1.03%) are configured as Distributed RAM, while no resources are allocated for latches or F7/F8 Muxes, indicating streamlined logic implementation. With an overall site utilization of just 8.29%, the design leaves substantial FPGA resources available for potential system expansions or additional features. These metrics confirm the hardware definition successfully achieves its objectives for real-time motor control and sensor data processing while maintaining low resource overhead, making it suitable for further development or integration with more complex systems.

6.3 Conclusion

1. The FPGA-based Electronic Speed Controller (ESC) and Inertial Measurement Unit (IMU) system have been successfully developed, integrating advanced sensors such as the MPU6050, BMP280, and HMC5883L with FPGA technology to ensure precise motor control and accurate sensor data acquisition. This integration results in a high-performance system suitable for a wide range of applications.
2. A Kalman filter was implemented in VIVADO SDK for sensor fusion, reducing noise and improving the accuracy of sensor data. The filter enhances system stability, ensures smoother sensor readings, and optimizes the control logic, thus boosting the overall performance of the system.
3. Real-time processing capabilities of the system allow for efficient motor control, enabling adaptive speed control and precise motion tracking. The integration of sensors with the FPGA allows for rapid data processing and timely adjustments in motor control, making the system highly responsive.
4. The system is tailored for applications requiring precise motion tracking and adaptive motor speed control, such as drones, robotics, and industrial automation. The combination of accurate sensor data and efficient motor control provides a robust solution for these dynamic fields.
5. The use of the XADC module for back-EMF detection via the FPGA ensures efficient BLDC motor control. The integration of zero-crossing detection with GPIO channels guarantees precise timing in the motor commutation process, enhancing the smoothness of motor operation.

6. The design of the ESC leverages a full-bridge 6-MOSFET motor driver configuration, ensuring reliable and efficient power delivery to the BLDC motor. This configuration supports high-current demands while maintaining efficient power conversion, critical for applications that require significant torque and speed.
7. The use of I2C communication protocols with modules like the ADS1115 and the HMC5883L ensures seamless sensor data transmission. The FPGA system handles multiple I2C channels efficiently, facilitating accurate sensor reading and communication without latency, which is crucial for real-time processing.
8. The project offers a scalable and customizable FPGA-based solution that provides researchers and developers with flexibility for further expansion or adaptation to different sensor configurations or control systems. It enables users to modify hardware and software components to meet specific application needs.
9. Improved system accuracy, reduced latency, and greater efficiency make this ESC and IMU system a reliable choice for high-performance control systems. The FPGA implementation ensures low-latency responses, which is critical for time-sensitive applications like autonomous vehicles and robotics.
10. The project not only provides an advanced solution for motor control and sensor data acquisition but also lays a foundation for future developments in FPGA-based control systems. The design's flexibility and performance position it as a valuable asset for further research, innovation, and commercialization in diverse fields such as robotics, aerospace, and industrial automation.

6.4 Future Scope

1. ESC Optimization: The ESC can be further optimized by refining back-EMF detection algorithms, and improving PWM control strategies to enhance motor efficiency, and response time. Implementing adaptive motor control techniques in VIVADO SDK can further reduce latency, and ensure precise speed regulation in real-time applications.
2. IMU Performance Enhancement: The IMU system can be improved by integrating higher-precision sensors or enhancing the existing Kalman filter to improve orientation estimation accuracy. Adding real-time error compensation can further refine motion tracking for drones, and robotics.
3. Improved Sensor Data Fusion: Enhancing the Kalman filter implementation by optimizing matrix computations or exploring alternative fusion methods (such as machine learning-

based sensor fusion) could further improve noise reduction, and system stability, leading to more accurate motion estimation.

4. Power Efficiency: Optimizing FPGA resource utilization in VIVADO SDK can help reduce power consumption, extending the battery life of UAVs, and embedded systems. Implementing dynamic power management techniques can improve energy efficiency without compromising performance.
5. ESC-IMU Integration: Improving the real-time interaction between ESC, and IMU by synchronizing motor control with sensor data feedback can enhance system adaptability. Implementing faster data exchange through efficient I2C, and UART communication protocols can ensure precise motor adjustments based on immediate motion data, improving stability in UAVs, and robotic applications.

Chapter 7

References

[1] J. A. Farrell, F. O. Silva, F. Rahman, and J. Wendel, “Inertial Measurement Unit Error Modeling Tutorial: Inertial Navigation System State Estimation with Real-Time Sensor Calibration,” *IEEE Control Systems Magazine*, vol. 42, no. 6, pp. 40–66, 2022, doi: 10.1109/MCS.2022.3209059.

[2] Z. Z. M. Kassas, M. Maaref, J. J. Morales, J. J. Khalife, and K. Shamei, “Robust Vehicular Localization and Map Matching in Urban Environments Through IMU, GNSS, and Cellular Signals,” *IEEE Intelligent Transportation Systems Magazine*, vol. 12, no. 3, pp. 36–52, 2020, doi: 10.1109/MITS.2020.2994110.

[3] D. Gayathri, P. Nishanthi, and K. S. Kumar, “Design and Performance Analysis of Electrical Vehicle Using BLDC Motor and Bidirectional Converter,” in *2021 2nd International Conference on Smart Electronics and Communication (ICOSEC)*, 2021, pp. 752–756. doi: 10.1109/ICOSEC51865.2021.9591901.

[4] P. Damodharan and K. Vasudevan, “Sensorless Brushless DC Motor Drive Based on the Zero-Crossing Detection of Back Electromotive Force (EMF) From the Line Voltage Difference,” *IEEE Transactions on Energy Conversion*, vol. 25, no. 3, pp. 661–668, 2010, doi: 10.1109/TEC.2010.2041781.

[5] A. Serrani, “Technical Committee on Nonlinear Systems and Control [Technical Activities],” *IEEE Control Syst*, vol. 45, no. 2, pp. 21–22, Apr. 2025, doi: 10.1109/MCS.2025.3534977.

[6] G. Como, “Networks and Communication Systems [Technical Activities],” *IEEE Control Syst*, vol. 45, no. 2, pp. 19–20, Apr. 2025, doi: 10.1109/MCS.2025.3534937.

[7] K. Y. Pettersen, N. Ozay, C. Johnsson, E. Westin, and M. Bauer, “Historical Women Influencers in Automatic Control [Member Activities],” *IEEE Control Syst*, vol. 45, no. 2, pp. 13–18, Apr. 2025, doi: 10.1109/MCS.2025.3534936.

[8] D. S. Bernstein, “The Frequency Domain [25 Years Ago],” *IEEE Control Syst*, vol. 45, no. 2, pp. 10–12, Apr. 2025, doi: 10.1109/MCS.2025.3534924.

[9] C. Beck, K. H. Johansson, and S. Mastellone, “Diversity, Outreach, and Development in the CSS [President’s Message],” *IEEE Control Syst*, vol. 45, no. 2, pp. 7–9, Apr. 2025, doi: 10.1109/MCS.2025.3534498.

[10] M. L. Hoang, M. Carratù, V. Paciello, and A. Pietrosanto, “Noise Attenuation on IMU Measurement For Drone Balance by Sensor Fusion,” in *2021 IEEE International Instrumentation and Measurement Technology Conference (I2MTC)*, 2021, pp. 1–6. doi: 10.1109/I2MTC50364.2021.9460041.

[11] P. L. Petrov, “IMU Sensor Fusion with Quaternion Interval-Based Orientation Filters Processed over Smartphone Scanned Data,” in *2023 XXXII International Scientific Conference Electronics (ET)*, 2023, pp. 1–5. doi: 10.1109/ET59121.2023.10279076.

[12] J.-H. Yoo and T.-U. Jung, “A Study on Output Torque Analysis and High Efficiency Driving Method of BLDC Motor,” in *2020 IEEE 19th Biennial Conference on Electromagnetic Field Computation (CEFC)*, 2020, pp. 1–4. doi: 10.1109/CEFC46938.2020.9451336.

[13] Digilent, “ZYBO Board,” Digilent. Accessed: Mar. 20, 2025. [Online]. Available: https://digilent.com/reference/programmable-logic/zybo/start

[14] InvenSense Inc., “MPU6050 Datasheet,” InvenSense Inc. Accessed: Oct. 12, 2024. [Online]. Available: https://invensense.tdk.com/wp-content/uploads/2015/02/MPU-6000-Datasheet1.pdf

[15] Bosch Sensortec, “BMP280 Datasheet,” Adafruit. Accessed: Oct. 12, 2024. [Online]. Available: https://cdn-shop.adafruit.com/datasheets/BST-BMP280-DS001-11.pdf

[16] Honeywell, “ HMC5883L Datasheet,” Honeywell. Accessed: Mar. 24, 2025. [Online]. Available: https://www.farnell.com/datasheets/1683374.pdf

[17] “BLDC Motors”, Accessed: Oct. 21, 2024. [Online]. Available: https://robu.in/product/bmp280-barometric-pressure-and-altitude-sensor-i2c-spi-module/

[18] Infineon, “IR2101 Datasheet,” Infineon. Accessed: Mar. 20, 2025. [Online]. Available: https://www.infineon.com/dgdl/Infineon-ir2101-DS-v01_00-EN.pdf?fileId=5546d462533600a4015355c7a755166c

[19] International Rectifier, “IRF3205 Datasheet,” Infineon Technologies. Accessed: Oct. 12, 2024. [Online]. Available: https://www.infineon.com/dgdl/Infineon-IRF3205-DataSheet-v01_01-EN.pdf?fileId=5546d462533600a4015355def244190a

[20] “Lipo Battery”, Accessed: Oct. 21, 2024. [Online]. Available: https://th.bing.com/th/id/OIP.vGLTr3Zv8Lm6wB8oH_Sh4gHaHa?rs=1&pid=ImgDetMain

[21] Xilinx, “Xilinx Vivado,” Xilinx. Accessed: Oct. 12, 2024. [Online]. Available: https://www.amd.com/en/products/software/adaptive-socs-and-fpgas/vivado.html